

METHODOLOGICAL STUDY OF READING PROCESSES WITH ERPs AND ER-fMRI

S. Casarotto*, A. M. Bianchi*, S. Cerutti*, N. Vanello[¶], E. Ricciardi[§], C. Gentili[§], L. Sani[§], D. Bonino[§], M. Guazzelli[†], P. Pietrini[§], L. Landini[‡] and G. A. Chiarenza**

* Dept. Biomedical Engineering, Polytechnic University of Milan, Milan, Italy

[¶] Dept. Electrical Systems and Automation, Faculty of Engineering, University of Pisa, Pisa, Italy

^{||} MRI Laboratory, Institute of Clinical Physiology, Council of National Research, Pisa, Italy

[‡] Dept. Information Engineering, University of Pisa, Pisa, Italy

[§] Lab. Clinical Biochemistry, Dept. Experimental Pathology, Univ. of Pisa Med. School, Pisa, Italy

[†] Dept. Psychiatry, Neurobiology, Pharmacology and Biotechnology, Univ. of Pisa Med. School, Pisa, Italy

** Dept. Child and Adolescent Neuropsychiatry, Az. Osp. "G. Salvini", Rho Hospital, Rho, Italy

silvia.casarotto@polimi.it

Abstract: The combined application of different investigating techniques is helpful for studying reading mechanisms, since they found on the integration among visual, auditory, motor, attentive and cognitive processes. Electrophysiological scalp recordings and functional magnetic resonance provide significantly correlated measures of brain function and are characterized by complementary spatiotemporal resolution. This work describes an event-related experimental design for studying grapheme-phoneme association mechanisms naturally active while reading. ERPs and fMRI were separately acquired from healthy volunteers during passive observation and overt reading of single letters and non-alphabetic symbols visually presented. Concatenated EEG single trials were pre-processed using Independent Component Analysis (ICA) decomposition: current density distribution inside the brain was estimated applying Low Resolution Electromagnetic Tomography (LORETA) to artefact-free independent components. Multiple regression with a set of triangular basis functions was performed for time series images analysis. LORETA and fMRI local maxima were considered functionally connected if they were not farther than 30 mm. Results of application to a single subject are presented as an example. The method is promising for the study of cognitive functions that involve complex brain networks, each working at different spatial and temporal scales.

Introduction

Written language is certainly a powerful means of sharing information and most of our knowledge is usually acquired through reading. Reading processes found on the integration among visual, auditory, motor, attentive and cognitive functions. Furthermore,

language structure markedly influences reading strategies: ambiguous grapheme-phoneme association rules usually implicate greater reading difficulties.

Complexity of brain networks involved in reading has forced researchers to apply different methodologies for describing the underlying mechanisms with enough details (1-8). Neuro-physiological recordings as electro- and magneto-encephalography and event-related potentials (EEG, MEG, ERPs) provide real-time measurements of electric and magnetic activity of the brain: their capability of localizing neural sources is limited by blurring effect due to scalp interposition between brain and sensors and by ambiguity of solution of the "inverse problem" (9,10). ERPs and EEG are less costly and easier to apply compared to MEG. Neuroimaging techniques as positron emission tomography (PET) and functional magnetic resonance (fMRI) indirectly quantify changes in metabolism and blood oxygenation due to neuronal activity with details of some mm: their temporal resolution is on the order of seconds because of the low-pass filtering characteristic of the hemodynamic response (11,12). fMRI is often preferred in comparison with PET since it is not invasive.

Animal studies have proved that the blood oxygenation level dependent (BOLD) signal of fMRI is an indirect indicator of neuronal activity and that the two measures have a significant overall concordance rate (13). Specifically, the BOLD contrast reflects the input and intra-cortical local processing of small neuronal populations (14). Therefore, it seems reasonable to combine electric and hemodynamic measures of brain activity for usefully exploiting their complementary spatiotemporal resolution. This work describes an experimental design for studying grapheme-phoneme association mechanisms naturally active during reading, which encompasses separate acquisition of ERPs and fMRI with the same stimulation protocol. We propose a mathematical approach to

integrate the information provided by the two methodologies.

Materials and Methods

ERPs Recording: EEG was recorded from 19 electrodes referred to right mastoid, integrated in an elastic cap and placed according to the standard 10-20 system. EOG was bipolarly recorded using 2 electrodes placed over and below the right eye. EEG and EOG recordings were band-pass filtered between 0.02-30 Hz and sampled at 256 Hz. For further analysis the sample rate was halved. Electromyographic activity of lips muscles was recorded for measuring the reading time. During the test, subjects were sitting in a dimly illuminated, electrically and acoustically shielded room and stimuli were displayed on a CRT screen.

fMRI Recording: Multi-slice echo-planar images (EPIs) were axially acquired on a 1.5 Tesla MRI scanner (GE Medical Systems Signa) with TE = 40 ms, TR = 2 s, FOV = 240 mm with 64 x 64 acquisition matrix and 22 contiguous 5-mm slices (3.75 mm x 3.75 mm in-plane resolution). Each functional run consisted of 115 brain volumes. In the same session, a high resolution structural scan was acquired in the sagittal plane using a 3D GRASS sequence with TE = 5.22 ms, TR = 12.1 ms, FOV = 240 mm with 256 x 256 acquisition matrix and 120 slices (0.94 x 0.94 x 1.2 mm voxel size). fMRI was recorded applying a rapid event-related (ER) design with jittered inter-stimulus interval (ISI) and randomised stimulus presentation. Head movements were limited by carefully placed constraints. Stimuli were projected onto a screen located near the bottom of the bore and viewed from a mirror mounted on the head coil.

Experimental Protocol: Stimulation was provided and regulated using Presentation® software (Version 0.76, <http://www.neurobs.com>). Stimuli consisted in white single characters (Italian capital and small letters and non-alphabetic symbols) visually presented for 5 ms on a black background. ISI was not shorter than 2 s and was randomly chosen as an integer multiple of 500 ms. One *passive* and one *active* condition were applied. The passive condition consisted in simply watching at isolated and randomly ordered letters and symbols. Trials were sorted *a posteriori* for estimating the specific responses to letters and symbols (labelled *letter presentation* LP and *symbol presentation* SP tasks). The active condition consisted in reading aloud the letters and was labelled *letter recognition* (LR) task. We used single isolated letters rather than words to prevent that high-level cognitive strategies as inferences from the context and semantic analysis could interfere with the primitive reading mechanisms, e.g. grapheme-phoneme association. We set a very short stimuli duration to force subjects paying great attention and using visual *gestalt* to perform the task. The randomised sequences of stimulus events were generated so that the overlapping hemodynamic responses could be disentangled with the least amount of unexplained variance. The same

stimulus ordering was applied to ERPs and fMRI. Only for ERPs, ISI was adjusted to obtain a minimum of 4 s. Data acquisition was partitioned into periods of continuous recording, labelled runs, each lasting about 4 min and containing 50 stimuli (25 letters and 25 symbols for passive condition and 50 letters for active condition). We estimated that 6 passive and 3 active runs provided enough data for satisfactory signal-to-noise (SNR) of averaged ERPs and statistical power of fMRI signal.

ERPs analysis: ERPs were computed for LP, SP and LR task separately by averaging a minimum of 40 trials, each lasting 2 s pre- and 2 s post-stimulus. Before averaging, ocular artefacts were reduced by applying the method described in (15).

Independent Component Analysis (ICA) decomposition was performed applying the *runica* algorithm as implemented in EEGLAB toolbox (16) (<http://sccn.ucsd.edu/eeeglab>). For each subject and task, the concatenated single trials time series was modelled as a linear combination of spatially fixed and temporally independent components (ICs):

$$\mathbf{x}(t) = \mathbf{A} \cdot \mathbf{s}(t) \quad (1)$$

where $\mathbf{s}(t) = [s_1(t) \ \cdots \ s_N(t)]^T$ collects the unknown ICs, $\mathbf{x}(t) = [x_1(t) \ \cdots \ x_M(t)]^T$ the EEG recordings for all M channels and \mathbf{A} ($M \times N$) contains unknown mixture coefficients. ICA algorithm searches for a linear transformation \mathbf{B} ($N \times M$):

$$\hat{\mathbf{s}}(t) = [s_1(t) \ \cdots \ s_N(t)] = \mathbf{B} \cdot \mathbf{x}(t) \quad (2)$$

so that the estimated components $\hat{\mathbf{s}}(t)$ are as independent as possible. In this work the independent sources were separated using information maximization (17). The number of estimated ICs was assumed to be equal to the number of recording channels ($M = N$): therefore 19 ICs were computed for each task and subject. Visual inspection of component scalp maps, time courses and spectral power plots was performed to reject possible artefact sources from further analysis. In particular, we discarded spatially localized components with spectral peaks at high frequencies because they likely represented muscular activity. Averaged ERPs were reconstructed from the retained ICs and compared with those computed before ICA decomposition, in order to verify that task-related cerebral activity was not altered by rejection of components. The contribution of each IC to averaged ERPs was computed and stored on disk.

The Low Resolution Electromagnetic Tomography (LORETA) method (18) (<http://www.unizh.ch/keyinst/NewLORETA/LORETA01.htm>) was applied to compute the three dimensional distribution of current density (mA/mm²) inside the brain from electrical scalp recordings. LORETA provides the “smoothest” linear solution to the inverse problem: solution space is restricted to grey matter and consists of 2394 voxels at 7-mm spatial resolution. The LORETA transformation matrix was computed using the electrode coordinates in

Talairach atlas (19) extracted from a standardized template included in the software and therefore was constant among subjects. Standardized LORETA source estimation was applied to averaged ERPs reconstructed using only one IC at a time, thus obtaining a list of local current density maxima for each IC: the first three maxima were used for studying correlation with activated regions in fMRI images.

fMRI analysis: The first 5 volumes of each functional run were discarded from statistical analysis. Images were analysed using Analysis of Functional Neuroimages (AFNI) software (20). Pre-processing steps of functional data included: slice timing correction with cubic interpolation for aligning dataset slices to the same time origin; registration of scans to a selected brain volume with 7th order polynomial interpolation for correcting rigid translations and rotations of the head; spatial smoothing with a 5-mm full-width high-maximum (FWHM) Gaussian filter for reducing noise and increasing functional overlap between runs and subjects; signal intensity normalization based on the average intensity in the brain for reducing global signal variability among subjects. All the 9 runs recorded from each subject were concatenated. *Multiple regression* was applied for time series images analysis: the hemodynamic response function (HRF) to a single event was modelled as a linear combination of 3 basis functions (Fig. 1).

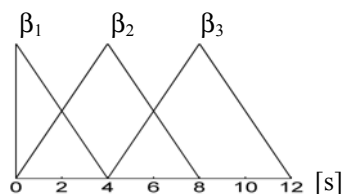


Figure 1: Time course of the ideal hemodynamic response to a single event occurring at 0 s.

The ideal hemodynamic response for each task was obtained by convolving the HRF with the corresponding stimulus timing, thus giving rise to 9 regressors of interest (3 basis functions x 3 stimulus categories). Baseline was separately modelled for each run as a 2nd order polynomial ($a+bt+ct^2$). The estimated movement parameters (3 for rotation and 3 for translation around xyz axes) were added as confounds. General linear tests (GLTs) were performed to identify active regions for each specific task. A double thresholding method was used: the t-test of the sum of regressor coefficients for each stimulus category versus baseline was thresholded at $P < 10^{-3}$ after masking with omnibus F-test thresholded at $P < 10^{-6}$. Clusters of suprathreshold voxels were built using nearest neighbours rule and 560 mm³ minimum size. Talairach coordinates of each cluster's local maximum were computed.

ERPs-fMRI integration: The Euclidean distance between the local maxima obtained from fMRI maps and LORETA images was computed for each task. The pairs of local maxima not farther than 30 mm, i.e. about

4 LORETA voxels, were considered meaningfully related and the LORETA signals at the corresponding coordinates were computed for estimating the time course of dynamic activation in those areas.

Results

The results described below refer to a single healthy subject analysis. Figure 2 shows the scalp maps and time courses of the first 4 artefact-free ICs for each task.

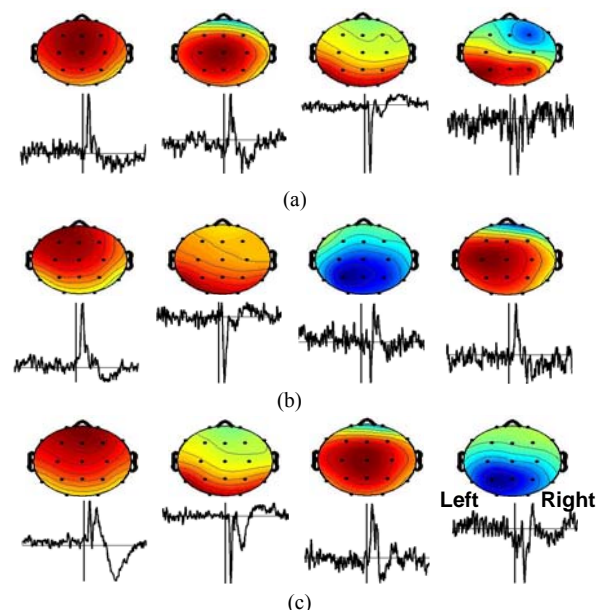


Figure 2: Scalp maps and time courses of the first 4 artefact-free ICs computed from (a) LP, (b) SP and (c) LR tasks.

Figure 3 shows 12 anatomical axial slices from $z = -17$ mm to $z = +60$ mm, 7-mm steps, with superimposition of functional activations, represented as colour-coded sum of regressor coefficients for significantly activated regions.

During letter presentation meaningful correspondence between LORETA and fMRI local maxima was observed in bilateral middle temporal and fusiform gyri (BA 19/22/37), right inferior parietal lobule (BA 39/40) and precuneus (Tab. 1). Additional fMRI activations were present in bilateral precentral gyrus (BA 6) and left middle/superior frontal gyrus (BA 8/9); additional LORETA maxima were found in left middle frontal gyrus (BA 10/11), bilateral middle temporal gyrus (BA 21) and superior temporal gyrus (BA 42 left and BA 38 right). During symbol presentation, adjacent local maxima between fMRI and LORETA were detected in left middle temporal and fusiform gyri (BA 19/39) (Tab. 2). fMRI analysis highlighted further activation of superior frontal gyrus (BA 6 bilaterally and BA 8 on the right) and left middle frontal gyrus (BA 6/9). The following LORETA maxima did not find any correspondence with fMRI: middle temporal gyrus (BA 21 bilaterally and BA 22 left), left middle frontal gyrus (BA 10), right superior temporal gyrus (BA 22/38/39) and right postcentral

gyrus (BA 40). Reading aloud task was characterized by many adjacent pairs of LORETA-fMRI local maxima: frontal (BA 6/7/31/32/45/47) and middle temporal (BA 20/21/22/37/39) gyri on the left hemisphere and middle frontal (BA 10/20/46), temporal (BA 21/22/37) and precentral (BA 3/4/9) gyri and inferior parietal lobule (BA 39/40) on the right. Additionally activated regions were detected with fMRI in left inferior/middle frontal and precentral gyri (BA 2/3/4/6/44/46); LORETA maxima were further present in right middle frontal (BA 10) and middle temporal (BA 21) gyri and precuneus.

Discussion

This study involved healthy volunteers: the investigation of reading functions in normal conditions is very helpful for better understanding and characterizing the alterations occurring in reading-impaired people and for developing specific rehabilitation treatments.

The experimental design described in this work has taken into account that participants were native Italian speakers. Word-rhyming tasks usually employed for investigating phonological processes (1-2,21-22) are not appropriate because Italian is a highly transparent language, characterized by perfect grapheme-phoneme matching. We considered that reading single letters allows to evaluate the simplest unit of grapheme-phoneme association mechanisms. Our approach can be defined *ecological*, since it reproduces in a laboratory as closely as possible the natural conditions of reading. The use of both letters and non-alphabetic symbols highlights the specificity of watching characters with linguistic content. Overt reading reveals the contribution of verbal-motor articulation to cerebral reading processes.

The event-related design applied to brain potentials was exactly reproduced in the fMRI session in order to make the measures comparable. This special attention for experimental conditions and parameters is fundamental for correctly integrating signals recorded with different modalities.

The mathematical approach proposed in this work is unusual and innovative. The application of more traditional analysis strategies on the same dataset, i.e. quantification of latency/amplitude/area of the main waves, would be interesting and useful for integrating and merging the results of both methods.

ICA method is able to estimate the statistically independent signals that have been linearly mixed into multichannel recordings. ICA decomposition was usefully employed for artefacts reduction, since extra-cerebral sources are independent from activity of interest.

Cognitive ERPs can be modelled as the projection on the scalp of spatially overlapping and temporally independent brain sources (10). However, they are characterized by marked morphological variability, which makes difficult and somewhat arbitrary to

identify temporally distinct waves associated to functionally specific stages of information processing.

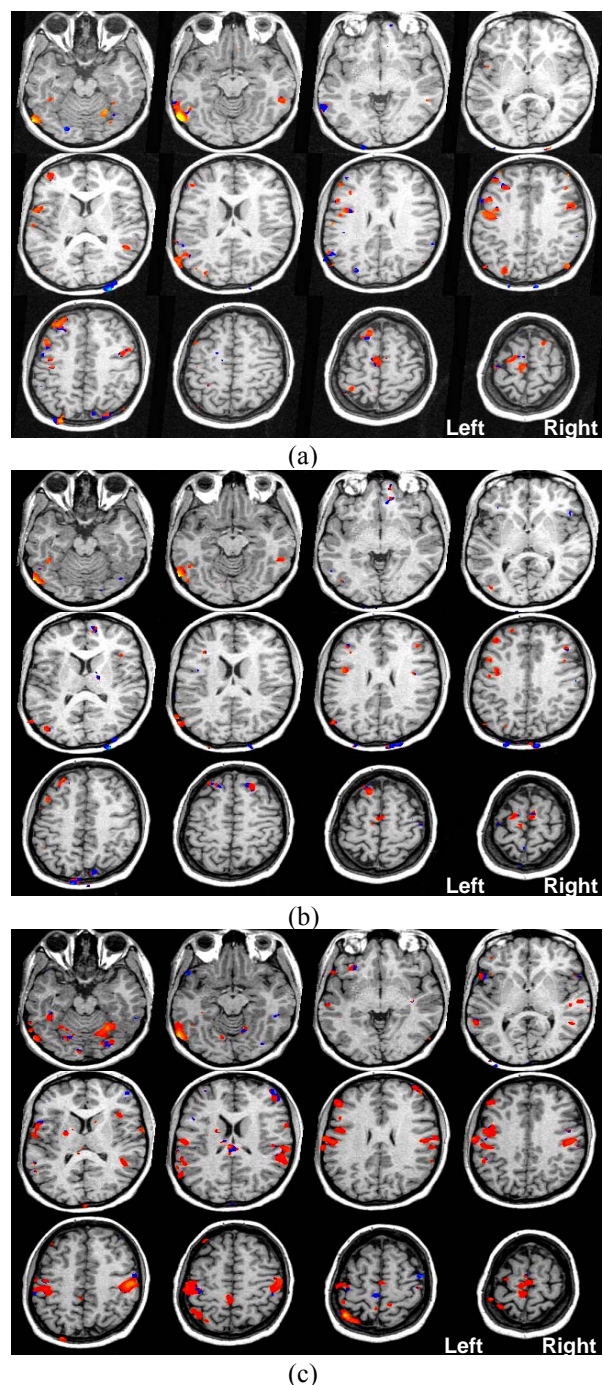


Figure 3: fMRI activations ($P < 10^{-3}$ after masking with omnibus F-test $P < 10^{-6}$) during (a) LP, (b) SP and (c) LR. Colours represent the sum of regressor coefficients.

Independent components extracted from EEG by means of ICA likely represent functionally specific neuronal networks, coherently activated by the event-related paradigm. Similarity of ICs scalp map, time course and spectral power density across subjects supports this assumption. Therefore, ICA decomposition is used here as a pre-processing step: current distribution in the brain is estimated applying LORETA to artefact-free ICs rather than to averaged ERPs.

Table 1: Approximate anatomical location and Talairach coordinates of LORETA and fMRI local maxima not farther than 30 mm during (a) LP, (b) SP and (c) LR tasks. BA = Brodmann's area.

Region (Talairach)	fMRI (x,y,z)	LORETA (x,y,z)
Left Middle Temporal Gyrus, Fusiform Gyrus (BA 19/22/37)	-56, -65, -12	-59, -39, 1
	-59, -63, 17	
Right Middle Temporal Gyrus, Inferior Parietal Lobule (BA 19/20/37/39)		53, -53, 15
	53, -39, -8	53, -60, -6
		53, -53, -13
Right Fusiform Gyrus, Inferior Parietal Lobule (BA 19/22/39/40)		53, -53, 15
	43, -71, 33	53, -53, 22
		53, -60, 15
Right Precuneus (BA 7/19/31)	23, -79, 36	4, -67, 22

(a)

Region (Talairach)	fMRI (x,y,z)	LORETA (x,y,z)
Left Middle Temporal Gyrus, Fusiform Gyrus (BA 19/39)	-56, -66, -13	-52, -60, 8
	-58, -68, 16	
	-42, -77, 12	-45, -67, 15
	-58, -68, 16	
	-42, -77, 12	

(b)

Region (Talairach)	fMRI (x,y,z)	LORETA(x,y,z)
Left Inferior Frontal Gyrus (BA 32/45/47)	-52, 19, 1	-52, 3, -20
Right Middle Frontal Gyrus (BA 10/20/46)	45, 44, 20	32, 52, 8
Left Middle-Superior Frontal Gyrus (BA 6/7)	-4, -18, 66	-3, -11, 64
	-4, -29, 61	
	-4, 1, 67	-3, -39, 50
	-4, -18, 66	
	-4, -29, 61	
Left Middle Frontal Gyrus (BA 31)	-4, -29, 61	-3, -46, 43
Left Middle Temporal Gyrus, Fusiform Gyrus (BA 20/21/22/37/39)	-59, -60, -13	-59, -39, 1
	-55, -46, 6	
	-40, -40, -14	-52, -60, 8
	-59, -60, -13	
	-55, -46, 6	
Right Middle Temporal Gyrus (BA 37)	25, -53, -17	53, -53, -13
Right Middle Temporal Gyrus (BA 21)	56, -19,0	53, 3, -13
Right Superior Temporal Gyrus (BA 22)	56, -19,0	60, -39, 8
	55, -34, 18	
	61, -26, 19	
Right Inferior Parietal Lobule (BA 40)	56, -19,0	60, -25, 22
	55, -34, 18	
	61, -26, 19	
	52, -15, 42	
Right Inferior Parietal Lobule (BA 39)	55, -34, 18	53, -53, 15
	61, -26, 19	
Right Precentral Gyrus (BA 3/4/9)	52, -15, 42	46, -32, 50
		46, 10, 36
Left Superior Parietal Lobule (BA 7)	-30, -46, 59	-3, -39, 50

(c)

The distribution of current density does not depend on the time frame but only on the IC used for LORETA estimation, since ICs have fixed spatial distribution. This approach associates each IC to a current density map, e.g. a list of local maxima: their coordinates in standard Talairach atlas indicate a set of functionally specialized regions that coherently activate independently from other, eventually partially overlapping, areas.

A potential source of results variability is attributable to the estimation of 3D spatial coordinates of electrodes from a standard template instead of their direct measurement: however, the elastic cap with integrated leads used in the experiment assured that inter-electrode distances were maintained constant despite subjects' head size.

Significant correlation between neurophysiology and BOLD signal has been shown by several studies (13-14): the main activation foci identified by the two methodologies are nearly the same. The distance between corresponding local maxima of activity is determined by the spatial resolution of both functional investigating techniques, besides the actual coupling between electrical and hemodynamic sources. A localization error on a single-subject basis of about 30 mm is acceptable, since LORETA voxel size is 7 mm³ and distinct Talairach transformations were used for LORETA (based on standard scalp) and fMRI (based on true subject brain). This observation is also supported by other studies (23-24).

In contrast to several researches (for a review see 9,10), in this work no *a priori* assumptions about the number and position of cerebral sources are made and solution of the inverse problem is not driven by fMRI activations: neurophysiological and functional neuroimaging signals are separately analysed and successively matched without mutual interferences. The main advantage of this approach lies in the possibility to fully study the regions coherently activated as well as those without correspondences between ERPs and fMRI, for hopefully finding physiologically meaningful interpretations.

Presentation of results was intentionally limited to application of the experimental procedure to a single subject, in order to stress the methodological approach rather than neurophysiological findings. The use of visually presented single letters for investigating brain functions is not frequent in literature (3,7,8); except for studies exploiting the complex graphic shape of Chinese and Japanese characters (2,25), most of the experimental procedures use words, pseudowords and letter strings (1,4-6,21-23,26). PET studies demonstrated that visual observation of words in contrast to letter strings specifically activates left medial extrastriate cortex and that reading aloud words recruits bilateral fusiform, superior temporal, precentral and inferior frontal gyri (5,6). Similar activations for attention to semantic and phonological relations were observed using fMRI in left inferior frontal cortex (BA 44/45), bilateral occipital cortex (BA 19), bilateral

fusiform and middle frontal gyri (BA6/37) and precuneus (BA7). Phonology showed greater activation than semantics in left inferior and precentral gyri (BA 6/44), right middle occipital gyrus (BA19) and bilateral inferior parietal lobule (BA 40) (22). Bimodal presentation of letters and speech sounds in congruent or incongruent combinations (7) revealed that grapheme-phoneme integration likely occurs in heteromodal superior temporal cortex. A recent study (8) showed that single-letter identification can be functionally isolated from other visual attributes of a pre-lexical stimulus (shape and colour): in fact, in contrast to symbol, letter viewing specifically activated BAs 47/37, while common activations were found in BA 6 and in more posterior regions (BA 19/39). Results from use of Chinese single characters replicate and extend those obtained in English (25): orthography to phonology transformation seems to be likely performed by left inferior frontal regions (BA 44/9/45/47), left supplementary motor area and left superior temporal lobe. Involvement of premotor cortex (BA 6) can be related to motor representation of letters. The physiological results presented in this study cannot be immediately generalized since they refer to a single subject. However, comparison with literature shows great concordance between our findings and those obtained by other researchers. Differences partially depend on stimulation parameters and timing. The novelty carried by the approach presented in this study lies in the possibility of integrating results from different investigating techniques, thus improving spatiotemporal resolution, since the study of cognitive functions cannot help facing the complex temporal dynamics of brain networks interaction.

References

- [1] BENTIN S., MOUCHETANT-ROSTAING Y., GIARD M. H., ECHALLIER J. F., and PERNIER J. (1999): 'ERP Manifestations of Processing Printed Words at Different Psycholinguistic Levels: Time Course and Scalp Distribution', *J. Cogn. Neurosci.*, 11(3), pp. 235-60
- [2] HUANG K., ITOH K., SUWAZONO S., and NAKADA T. (2004): 'Electrophysiological Correlates of Grapheme-Phoneme Conversion', *Neurosci. Lett.*, 366, pp. 254-8
- [3] TARKIAINEN A., HELENIUS P., HANSEN P. C., CORNELISSEN P. L., and SALMELIN R. (1999): 'Dynamics of Letter String Perception in the Human Occipitotemporal Cortex', *Brain*, 122, pp. 2119-31
- [4] SIMOS P. G., BREIER J. I., FLETCHER J. M., BERGMAN E., and PAPANICOLAOU A. C. (2000): 'Cerebral Mechanisms Involved in Word Reading in Dyslexic Children: a Magnetic Source Imaging Approach', *Cereb. Cortex*, 10, pp. 809-16
- [5] PETERSEN S. E., FOX P. T., SNYDER A. Z., and RAICHEL M. E. (1990): 'Activation of Extrastriate and Frontal Cortical Areas by Visual Words and Word-Like Stimuli', *Science*, 249, pp. 1041-44
- [6] BRUNSWICK N., MCCRORY E., PRICE C. J., FRITH C. D., and FRITH U. (1999): 'Explicit and Implicit Processing of Words and Pseudowords by Adult Developmental Dyslexics', *Brain*, 122, pp. 1901-17
- [7] VANATTEVELDT N., FORMISANO E., GOEBEL R., and BLOMERT L. (2004): 'Integration of Letters and Speech Sounds in the Human Brain', *Neuron*, 43, pp. 271-82
- [8] FLOWERS D. L., JONES K., NOBLE K., VANMETER J., ZEFFIRO T. A., WOOD F. B. and EDEN G. F. (2004): 'Attention to Single Letters Activates Left Extrastriate Cortex', *NeuroImage*, 21, pp. 829-39
- [9] VANOOSTEROM A. (1991): 'History and Evolution of Methods for Solving the Inverse Problem', *J. Clin. Neurophysiol.*, 8, pp. 371-80
- [10] BAILLET S., MOSHER J. C., and LEAHY R. M. (2001): 'Electromagnetic Brain Mapping', *IEEE Signal Processing Mag.*, 18, pp. 14-30
- [11] VOLKOW N. D., ROSEN B. and FARDE L. (1997): 'Imaging the Living Human Brain: Magnetic Resonance Imaging and Positron Emission Tomography', *Proc. Natl. Acad. Sci. USA*, 94, pp. 2787-8
- [12] MENON R. S., GATI J. S., GOODYEAR B. G., LUKNOWSKY D. C., and THOMAS C. G. (1998): 'Spatial and Temporal Resolution of Functional Magnetic Resonance', *Biochem. Cell. Biol.*, 76, pp. 560-71
- [13] DISBROW E. A., SLUTSKY D. A., ROBERTS T. P. L., and KRUBITZER L. A. (2001): 'Functional MRI at 1.5 Tesla: a Comparison of the Blood Oxygenation Level-Dependent Signal and Electrophysiology', *Proc. Natl. Acad. Sci. USA*, 97, pp. 9718-23
- [14] LOGOTHETIS N. K., PAULS J., AUGATH M., TRINATH T., and OELTERMANN A. (2001): 'Neurophysiological Investigation of the Basis of the fMRI Signal', *Nature*, 412, pp. 150-7
- [15] CASAROTTO S., BIANCHI A. M., CERUTTI S., and CHIARENZA G. A. (2004): 'Principal Component Analysis for Reduction of Ocular Artefacts in Event-Related Potentials of Normal and Dyslexic Children', *Clin. Neurophysiol.*, 115(3), pp. 609-19
- [16] DELORME A. and MAKEIG S. (2004): 'EEGLAB: an Open Source Toolbox for Analysis of Single Trial EEG Dynamics Including Independent Component Analysis', *J. Neurosci. Methods* 134: 9-21
- [17] BELL A. J. and SEJNOWSKI T. J. (1995): 'An Information-Maximization Approach to Blind Separation and Blind Deconvolution', *Neural Comput.* 7: 1129-59
- [18] PASCUAL-MARQUI R. D., MICHEL C. M. and LEHMANN D. (1994): 'Low Resolution Electromagnetic Tomography: a New Method for Localizing Electrical Activity in the Brain', *Int. J. Psychophysiol.* 18: 49-65

- [19] TALAIRACH J. and TOURNOUX P. (1988): 'Co-Planar Stereotaxic Atlas of the Human Brain', Thieme, Stuttgart
- [20] COX R. W. (1996): 'AFNI©: Software for Analysis and Visualization of Functional Magnetic Resonance Neuroimages', *Comput. Biomed. Res.* 29: 162-173
- [21] GROSSI G., COCH D., COFFEY-CORINA S., HOLCOMB P. J. and NEVILLE H. J. (2001): 'Phonological Processing in Visual Rhyming: a Developmental ERP Study', *J. Cogn. Neurosci.* 13(5): 610-25
- [22] MCDERMOTT K. B., PETERSEN S. E., WATSON J. M. and OJEMANN J. G. (2003): 'A Procedure for Identifying Regions Preferentially Activated by Attention to Semantic and Phonological Relations Using Functional Magnetic Resonance Imaging', *Neuropsychologia* 41: 293-303
- [23] VITACCO D., BRANDEIS D., PASCUAL-MARQUI R. and MARTIN E. (2002): 'Correspondence of Event-Related Potential Tomography and Functional Magnetic Resonance Imaging During Language Processing', *Hum. Brain Mapp.* 17: 4-12
- [24] MULERT C., JÄGER L., SCHMITT R., BUSSFELD P., POGARELL O., MÖLLER H.-J., JUCKEL G. and HEGERL U. (2004): 'Integration of fMRI and Simultaneous EEG: Towards a Comprehensive Understanding of Localization and Time-Course of Brain Activity in Target Detection', *NeuroImage* 22: 83-94
- [25] TAN L. H., FENG C.-H., FOX P. T. and GAO J.-H. (2001): 'An fMRI Study with Written Chinese', *NeuroReport* 12(1): 83-8
- [26] FIEZ J. A. and PETERSEN S. E. (1998): 'Neuroimaging Studies of Word Reading', *Proc. Natl. Acad. Sci USA* 95: 914-21